Journal of Engineering and Technological Advances (JETA)
https://jeta.segi.edu.my/index.php/segi
2025 Vol. 10 No. 1

DECOLORIZATION OF RICE BRAN OIL USING COCONUT SHELL-DERIVED ACTIVATED CARBON

[1,2]S M Anisuzzaman[*], [2]Maryam Faozi Mahfoudh Basowaidan

[1]Energy and Materials Research Group, Universiti Malaysia Sabah, UMS Road, 88400, Kota Kinabalu, Sabah, Malaysia

[2]Chemical Engineering Program, Faculty of Engineering, Universiti Malaysia Sabah, UMS Road, 88400, Kota Kinabalu, Sabah, Malaysia

[*]Corresponding Author: anis_zaman@ums.edu.my TEL: (60)-0168237107

Received: 23 May 2025; Accepted: 20 June 2025; Published: 30 June 2025
doi: 10.35934/segi.v10i1.133

Highlight:

~ Color pigment was successfully removed from crude rice bran oil (CRBO) by coconut shell-derived activated carbon (CSAC).

~ Assessing the effect of multiple adsorption parameters on the decolorization efficiency of CRBO using CSAC via response surface methodology (RSM).

~ Evaluate color measurements of oil samples after decolorization.

Abstract: This study focused on maximizing the removal of color pigments from crude rice bran oil (CRBO) using coconut shell-derived activated carbon (CSAC). The study began by analyzing the physical properties of the CSAC used, including pH, bulk density, moisture content, ash content, and iodine number. The analysis showed a pH of 6.95, bulk density of 0.68 g/mL, moisture content of 4.13%, ash content of 8.75%, and an iodine number of 851.84 mg/g. Response surface methodology (RSM) was applied to guide the decolorization process of the CRBO, using the identified conditions to treat the oil. The design variables included adsorbent dosage, temperature, and contact time, with decolorization efficiency serving as the actual and predicted response variable. With a composite desirability score of 0.929, the optimum predicted percentage for decolorization efficiency was determined to be 65.4% at 0.85% w/v, 50^{o}C, and a contact time of 43 min. Statistical analysis confirmed the significance of the optimization model. Based on the color analysis, it was determined that sample 1, which achieved the highest decolorization efficiency (61.1%), was the most successful decolorization process out of all the runs that have been conducted.

Keywords**:** rice bran oil; decolorization; activated carbon; response surface methodology; optimization

1. Introduction

Widely consumed in Asian nations, rice bran oil (RBO) is notable for its health advantages, including its regulated fatty acid composition, sterol, oryzanol, and vitamin E richness, which have earned it a ranking among the top three most nutritious edible oils by the World Health Organization (Liu *et al.*, 2019). The numerous biological functions of RBO include decreasing cancer growth, reducing cholesterol, and treating and preventing hypertension (Punia *et al.*, 2021; Phannasorn *et al.*, 2022). RBO is extracted from rice bran and subsequently refined through a variety of physical and chemical procedures that include several critical steps. Bran particles are either filtered or settled, followed by degumming, dewaxing, deacidification, bleaching, and deodorization (Tong & Bao, 2019). During decolorization, the oil is treated with an adsorbent substance, such as activated clay or activated carbon (AC), to eliminate color pigments, residual phospholipids, metals, and other contaminants that might shorten the oil's shelf life, give it an odd taste, and affect its overall quality. Crude rice bran oil (CRBO), like other edible oils, can contain contaminants that alter its color and quality. Various pigments, including chlorophyll-a and carotenoids, give the oil an unattractive color (Aung & Thiravetyan, 2014). Edible oil decolorization can be achieved through various techniques, including adsorption, chemical treatment, physical refining, membrane filtration, ultrafiltration, and enzymatic treatment (Worasith *et al.,* 2011). Among these, adsorption is regarded as the most common and effective method due to its efficiency in removing color pigments and other impurities.

AC is one of the most widely used adsorbents in such processes. For this study, coconut shell-derived activated carbon (CSAC) has been chosen for several reasons. CSAC typically has a high surface area, providing more active sites for adsorption and enhancing its decolorization efficiency (Ikumapayi *et al.*, 2020). Coconut shells are a renewable and abundant resource, making CSAC an environmentally friendly and sustainable option (Somashekhar *et al.*, 2018). Additionally, CSAC is cost-effective compared to other sources of AC and is chemically stable, allowing for regeneration and reuse multiple times, reducing overall costs and environmental impact (Punsuwan *et al.*, 2015; Ofulue *et al.*, 2020; Guliyev *et al.*, 2018). According to Ghahjaverestani *et al.* (2022), CSAC is more effective than commercial bleaching earth in reducing color and the greatest reductions in carotenoid (84.25%) and chlorophyll (82.30%) contents in soybean oil. Additional studies by Ofulue *et al.* (2020) and

Butt *et al*. (2020) have explored the use of various naturally sourced AC for decolorizing different edible oils.

Response surface methodology (RSM) was implemented in this study as it is crucial for optimizing the decolorization process. RSM is an approach that has gained popularity among modeling methodologies for relating the analysis between controllable factors and the response of interest. This may be demonstrated by contrasting RSM with the Taguchi approach, another well-liked optimization technique. However, the RSM method helps figure out optimization and the best conditions to get a high yield at a low cost. The findings of this study demonstrate the value of modeling and optimization in defining adsorption process variables and getting relevant knowledge about the physical properties of both the CSAC and produced oil in decolorization processes. The parameters optimized in this study include adsorbent dosage of CSAC (X_1), temperature (X_2), and contact time (X_3). The selected parameters demonstrated effective adsorption, ensuring a balance between sufficient active sites, process efficiency, and maintenance of oil quality (Damayanti *et al*., 2023; Sun *et al.*, 2023; Rekha *et al.*, 2014). These criteria were selected to provide comprehensive data on the decolorization process and cover a wide range of scenarios. Additionally, a three-factor, three-level central composite design (CCD) was used to identify the optimal conditions for decolorizing CRBO with CSAC.

2. Materials and methods

2.1 Raw material

Fresh CRBO was supplied by an RBO producing company in Bangladesh. As for the adsorbent, CSAC was purchased from a supplier located in Perak, Malaysia. The CSAC is available in granular form with particle sizes ranging from 2 to 4 mm.

2.2 Purification of CRBO and CSAC

An initial step before the decolorization process was the oil purification, which was done using the water degumming method. Firstly, 150 g of CRBO was heated to 95^{o}C. Then, deionized water (5 w/w%) was added to the oil and stirred by magnetic stirring at 250 rpm for 30 min. The degummed oil was then centrifuged at 3,000 rpm for 15 min (Paisan *et al.,* 2017; Engelmann *et al.,* 2016). As an extra purification step, the CSAC was submerged in hot distilled water for two hours before being rinsed with cold distilled water. Following that, the CSAC was dried for 24 h at 80°C in an oven and cooled down in a desiccator (Tan *et al.*, 2017).

2.3 Characterization of CSAC

The following physical characteristics of the CSAC were assessed: pH, bulk density, moisture content, ash content, and iodine number. It is essential to comprehend these qualities since they affect the quality of adsorption of the AC for the removal of color pigments from the CRBO. The CSAC sample was mixed with water, the solution was stirred well, and the pH was determined using a Mettler Toledo pH meter.

2.3.1 Determination of bulk density

To determine the bulk density of the CSAC sample, the first step was to set up an analytical balance with a 10 mL measuring cylinder. The measuring cylinder was filled with CSAC until the 10 mL mark was reached. The mass of carbon was indicated by the weight shown on the analytical balance. Equation 1 was used to determine the bulk density (Efeovbokhan *et al.*, 2019).

$$Bulk\ density = \frac{Mass\ of\ activated\ carbon,\ \ g}{Volume\ of\ measuring\ cylinder,\ \ mL} \quad (1)$$

2.3.2 Determination of moisture content

To determine the moisture content of the CSAC sample, 1.0 g of CSAC was dried in an 110°C oven for 3 h and cooled in a desiccator before weighing. The process of heating, cooling, and weighing was repeated until a constant mass of CSAC was achieved. Moisture content was calculated using equation 2 (Jeyakumar & Chandrasekaran, 2014).

$$Moisture\ content, \% = \frac{W_i - W_f}{W_i} \times 100 \quad (2)$$

where $W_i(g)$ is the initial mass of the activated carbon before drying and $W_f(g)$ is the final mass of the activated carbon after drying.

2.3.3 Determination of ash content

The determination of ash content was done by weighing CSAC after the moisture content test in a muffle furnace at 600°C for 4 h. Then, the ash was cooled in a desiccator before re-weighing. Ash content was calculated using equation 3.

$$Ash\ content, \% = \frac{W_3 - W_1}{W_2 - W_1} \times 100 \quad (3)$$

where $W_1(g)$ is the weight of empty crucible, and $W_2(g)$ is the weight of empty crucible and the activated carbon sample before furnace. $W_3(g)$ is the weight of crucible and the ash after furnace.

2.3.4 Determination of iodine number

0.2 g of CSAC was put into a 250 mL Erlenmeyer flask equipped with a ground glass stopper. 10 mL of 5% HCl solution was added into the flask and swirled gently. The stopper was loosened, and the sample was heated to boil for 30 s. The sample was then removed and cooled at room temperature. 100 mL of 0.1 N iodine solutions were pipetted into the flask and shaken vigorously for 30 s. The mixture was filtered using filter paper (Whatman number 2v). The first 30 mL of the filtrates were used to rinse the pipette. The filtrate was swirled, and 50 mL of it was pipetted into a clean 250 mL Erlenmeyer flask. The filtrate was titrated with 0.1 N sodium thiosulfate ($Na_2S_2O_3$) solutions until the solution turned yellow. 2 mL of starch indicator was added, and the titration continues until the solution turns colorless. The volume of $Na_2S_2O_3$ used was recorded. The iodine number ($\frac{X}{M}$) per gram of carbon was calculated using equation 4.

$$Iodine\ number\ \left(\frac{X}{M}\right) = \frac{A-(DF)(B)(S)}{M} \quad (4)$$

where, A = (N_2) iodine (12693.0); N_2 = iodine (N) = 0.1 N; DF = dilution factor = (100+10)/50 = 2.2; B = (N_1)(126.93); N_1 = $Na_2S_2O_3$ (N) = 0.1N; S = $Na_2S_2O_3$ (mL)

The second titration with the $Na_2S_2O_3$ was done in order to detect the present of iodine. The blue-black color solution was turned into color less when there was no iodine present in the solution. This total amount of $Na_2S_2O_3$ used in order to change the color of the solution to colorless was recorded to calculate the iodine number for the sample (Siragi *et al.*, 2021).

2.4 Response surface methodology (RSM) analysis

RSM was used to interpret and optimize three significant operating variables, including adsorbent dosage, temperature, and contact time, to obtain the best decolorization efficiency surface response of the RBO using CSAC. The adsorbent dosage, temperature, and contact time were restricted to 0.4 and 1.2% w/v, 50 to 110°C, and 20 to 60 min, respectively. These parameters were selected to collect thorough information on the decolorization efficiency and effective adsorption process. The best conditions for the RBO decolorization process can be determined by examining the connection between these process variables and the response variable, which improves process effectiveness. The operating variables and their ranges in this study were chosen based on existing literature by Damayanti *et al.* (2023), which focused on optimizing the carotenoid content removal in RBO. The selected ranges demonstrated effective adsorption within these limits, ensuring a balance between sufficient active sites,

process efficiency, and maintenance of oil quality. However, while the previous study primarily targeted carotenoid content, this study aims to investigate decolorization efficiency percentage as the response. This approach addresses the gap in existing literature, providing new insights into the effectiveness of these specific conditions for RBO decolorization. An overview of the coded values for the process parameters is shown in **Table 1**.

Table 1. Coded values of process parameters and corresponding responses

Symbol	Parameter	Units	Coded variable and level				
			$-\alpha$	Level -1	Level 0	Level 1	$+\alpha$
X_1	Dosage of absorbent	% w/v	0.1	0.4	0.8	1.2	1.5
X_2	Temperature	°C	29.6	50	80	110	130.5
X_3	Contact time	minute	6.4	20	40	60	73.6
Y	Decolorization efficiency	%		-	-	-	

2.5 Decolorization of RBO

Batch decolorization tests were conducted to evaluate the model under various operating situations using the proposed central composite design (CCD). The decolorization efficiency of the oil by CSAC was calculated using equation 5 (Worasith *et al.*, 2011).

$$Decolorization\ efficiency, \% = \frac{A_i - A_1}{A_i} \times 100 \quad (5)$$

where A_i is the initial absorbance value before the decolorization process at 410 nm, and A_1 is the absorbance value after the decolorization process at 410 nm.

2.6 Color analysis

Color analysis is critical for characterizing the oil in decolorization studies. Color analysis characterization was carried out utilizing a Hunterlab USA ColorFlex D65/100 colorimeter. Representative samples of RBO, designated as Sample 1 to Sample 7, were prepared before the examination. These samples were put into seven different 70 mL cups, and each cup was placed on the sample holder's measuring area. The colorimeter gave the colorimetric data when the measurement was finished. The colorimeter identifies three main color parameters. These parameters indicate the sample's brightness (L^*) and color opponent axes (a^* and b^*) where a^* values imply red to green. b^* values correlate to the yellowness or the blueness of the samples.

3. Results and discussion

3.1 Characterization of CSAC

Table 2 shows the findings of the physical examination for CSAC.

Table 2. Summary of the determined physical characteristics of CSAC

Properties	Value
pH	6.95
Bulk density, g/cm^3	0.68
Moisture content, %	4.13
Ash content, %	8.75
Idoine number, mg/g	851.84

Overall, the physical characteristics of the CSAC determined in this study all fall within acceptable ranges indicative of effective activated carbon for adsorption applications. As shown in **Table 2**, the pH value determined was nearly neutral, making it suitable for interacting with various dye molecules and improving adsorption efficiency (El Haddad *et al.*, 2013). Then for bulk density, the obtained value of 0.68 g/cm³ suggests a balanced porosity and surface area, which is crucial for the effective adsorption of color pigments (Dąbrowski *et al.*, 2005). Generally, the higher the bulk density, the more carbon material per unit volume; it may lower porosity and surface area, which in turn reduces the number of active adsorbed sites. On the other hand, a lower bulk density usually correlates with higher porosity and surface area. A moisture content of 4.13% aligns with the required ASTM D2867-09 standards, indicating high porosity and surface area for effective adsorption, as it specifies that the moisture content of the AC must be between 3 to 8% to obtain an optimum adsorption capacity. Zulkania *et al.* (2018) have also found that, depending on the activation process and precursor used the moisture content of AC derived from different agricultural by-products ranged from 5 to 7%. The ash content of 8.75% is within the acceptable limit of below 10%, ensuring minimal blockage of adsorption sites and maintaining the carbon's adsorption capacity. Lastly, the iodine number of 851.84 mg/g, which falls in the typical range of 500 to 1200 mg/g, reflects a high degree of microporosity, which is vital for the adsorption of small

molecules, thus making CSAC highly effective in purifying oils and removing contaminants (Mopoung *et al.*, 2015).

3.2 Responses obtained from adsorption using RSM

The design of experiments (DOE) constructed to plan the experimental run with the desired range of each factor and their respective levels are shown in **Table 3**.

The Design Expert version 13 programme under CCD was used to identify and determine the correlation between the response surface and the variables. The regression statistics for different models are provided in **Table 4**. As shown in **Table 4**, the R^2 value for the linear model is the least, followed by the Two-Factor Interaction (2FI) model. The quadratic model has adjusted R^2 of 0.765. Consequently, the RSM suggests the quadratic model for this study, while the cubic model is aliased in the removal efficiency, which can be attributed to the three independent variables.

The quadratic model was suggested for the RBO decolorization and the resulting model in terms of coded variables is as follows:

$$Y_2 = 47.30 + 1.66X_1 - 5.21X_2 + 6.41X_3 + 0.2587X_1X_2 + 2.03X_1X_3 + 3.40X_2X_3 - 6.73{X_1}^2 + 4.59{X_2}^2 - 10.03{X_3}^2 \quad (6)$$

where, Y_2 is the predicted decolorization efficiency, X_1, X_2, and X_3 correspond to the linear factor effect of dosage of adsorbent (w/v%), temperature (°C) and contact time (min).

The coefficient of an independent variable is positive, which means that there is a direct relationship between the independent variable and the dependent variable. While a negative coefficient signifies an impact of an inverse relationship, in which the independent is being increased, the dependent will be decreased. Furthermore, a positive sign preceding a term has a synergistic impact, while a negative sign preceding a term has an antagonistic effect. The generated model's effectiveness was assessed using the correlation coefficient value. The R^2 value suggests that 87.6% of the variance in the response variable can be attributed to the cause's effects, leaving 12.4% of the variation unpredictable and unexplained.

Table 3. Design of experiment for three independent variables and experimental results

Run	CSAC dosage, X_1	Temperature, X_2	Contact time, X_3	Experimental decolorization efficiency, Y_1	Predicted decolorization efficiency, Y_2

1	0.8	80.0	40.0	47.5	47.3
2	1.2	50.0	60.0	57.3	46.8
3	0.8	80.0	6.4	9.1	8.2
4	0.8	80.0	40.0	47.5	47.3
5	0.8	80.0	40.0	47.5	47.3
6	1.2	110.0	60.0	48.8	43.7
7	0.8	80.0	73.6	22.0	29.7
8	0.8	30.0	40.0	61.1	69.0
9	1.2	50.0	20.0	42.0	36.7
10	0.1	80.0	40.0	30.6	25.5
11	0.4	110.0	60.0	35.3	35.8
12	1.2	110.0	20.0	23.0	20.0
13	0.8	130.5	40.0	52.7	51.5
14	0.4	110.0	20.0	14.5	20.2
15	0.8	80.0	40.0	47.5	47.3
16	0.8	80.0	40.0	47.5	47.3
17	1.5	80.0	40.0	19.1	31.1
18	0.8	80.0	40.0	47.5	47.3
19	0.4	50.0	20.0	37.6	38.0
20	0.4	50.0	60.0	41.7	40.0

Table 4. Regression statistics for decolorization efficiency, Y_1

Source	Standard deviation	R^2	Adjusted R^2	Predicted R^2	Comment
Linear	13.930	0.238	0.095	-0.311	
2FI	15.130	0.269	-0.069	-0.522	

Quadratic	7.100	0.876	0.765	0.060	Suggested
Cubic	4.370	0.972	0.911	-5.195	Aliased

3.3 Statistical analysis

Determining the relevance and validity of the produced model heavily relies on the ANOVA model component. The results of the variance analysis (ANOVA) for the quadratic response surface model are shown in **Table 5**.

Table 5. ANOVA for regression model

Source	Sum of square	DF	Mean square	F-value	P-value	Remarks
Model	3568.2	9.0	396.5	7.9	0.0017	significant
X_1	37.5	1.0	37.5	0.7	0.4083	
X_2	370.4	1.0	370.4	7.4	0.0218	
X_3	560.7	1.0	560.7	11.1	0.0075	
X_1X_2	0.5	1.0	0.5	0.0	0.9199	
X_1X_3	33.1	1.0	33.1	0.7	0.4364	
X_2X_3	92.6	1.0	92.6	1.8	0.2050	
${X_1}^2$	652.9	1.0	652.9	13.0	0.0048	
${X_2}^2$	303.2	1.0	303.2	6.0	0.0340	
${X_3}^2$	1448.6	1.0	1448.6	28.8	0.0003	
Residual	503.52	10.00	50.35			
Lack of fit	503.52	5.00	100.70			
Pure error	0.00	5.00	0.00			
Cor. total	4071.68	19.00				

According to **Table 5**, the F-value was 7.9, indicating that the regression equation can account for a significant portion of the response variation. In the meantime, the P-value is used to determine the statistical significance of the F-distribution. When the P-value is less than 0.05, the model is considered statistically significant. In this study, the P-value was 0.0017, which is considerably less than 0.05.

3.4 Interpretation of the response surface plots

To examine the effects of three process parameters on the decolorization effectiveness of the various oil samples employing CSAC adsorbent, 2D and 3D surface plots were generated.

3.4.1 Effect of adsorbent dosage and temperature

The relationship between decolorizing temperature and CSAC loading and RBO decolorization efficiency is shown in **Figure 1 (a,b)**.

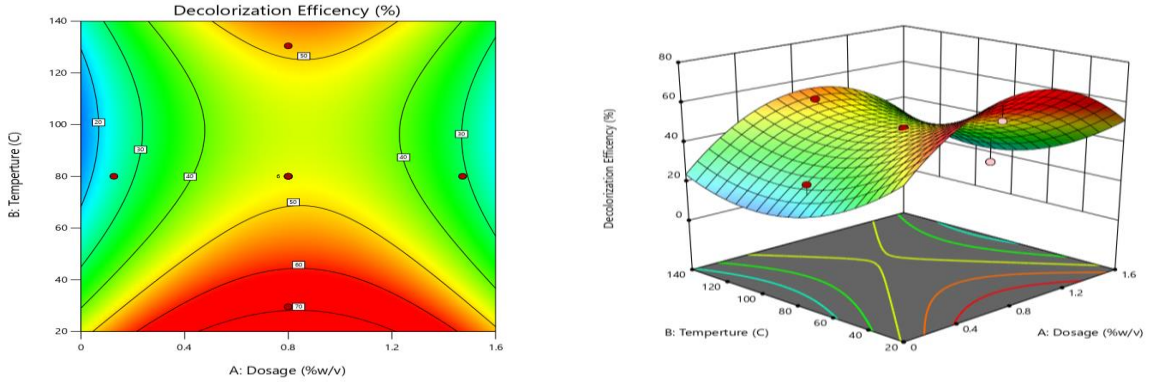

(a) (b)

Figure 1. (a) Contour plot interaction between dosage ($X1$) and temperature ($X2$) (b) 3D Surface Plot of response interaction between dosage ($X1$) and temperature ($X2$)

The highest decolorization efficiency percentages were produced at a temperature of 20-40°C and an AC dosage between 0.4-0.8% w/v. These conditions are indicated in red. Similarly, a temperature of 120-140°C and a high AC loading of 1-1.2% w/v produced a high percentage of decolorization efficiency. According to Chetima *et al.* (2018), the decolorizing temperature and the adsorbent loading (w/v) are directly correlated. Carotene is a specific type of carotenoid and is a pigment that is highly present in the RBO and is a thermolabile color pigment (Guliyev *et al.*, 2018). Moreover, the greatest decolorization efficiency was achieved at temperatures between 30 and 100°C with a CSAC content of 0.4-0.8% w/v, as shown by **Figure 1 (a,b)**.

3.4.2 Effect of contact time and temperature

As can be observed in **Figure 2 (a,b)**, the red area represents the largest decolorization % for temperatures between 30 and 80°C. The efficiency percentage obtained at 20-50°C is rather low since longer contact times are necessary to achieve larger percentages. According to Ifa *et al.* (2021), a longer adsorption time is also required to obtain the ideal carotene content when the temperature rises. In addition, higher temperatures and longer heating times will speed up the reaction rate because they encourage more active particle movement and collisions. The collision is larger when the temperature is higher. As a result, the adsorbent's capacity to

absorb contaminants will likewise rise (Gao & Fatehi, 2018). Nevertheless, Pohndorf *et al.* (2016) found that utilizing an excessively high temperature can result in oxidation and decrease the oil's efficacy; hence it is advised against decolorization at high temperatures (Pohndorf *et al.*, 2016; Rahman *et al.*, 2019).

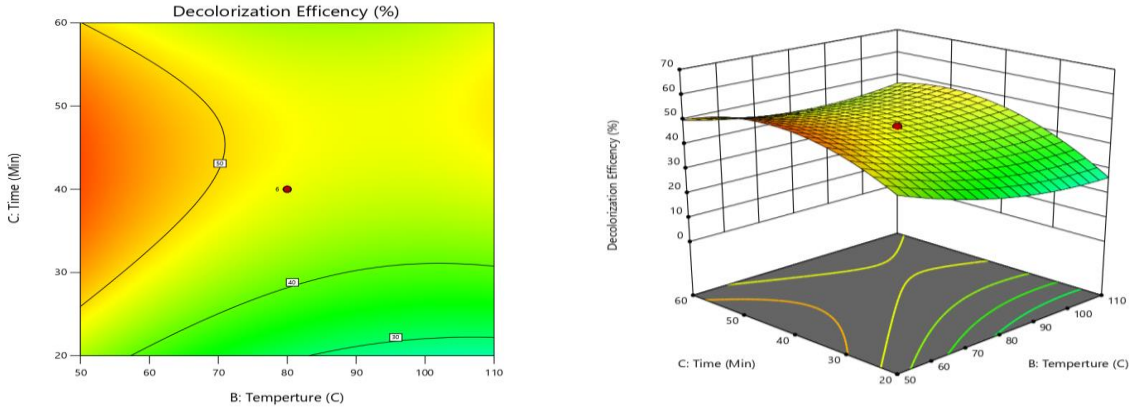

(a) (b)

Figure 2. (a) Contour plot interaction between temperature ($X2$) and contact time ($X3$) (b) 3D Surface Plot of response interaction between temperature ($X2$) and contact time ($X3$)

3.4.3 Effect of adsorbent dosage and contact time

Figure 3 (a,b) illustrates the best decolorization percentage, indicated as a green region turning yellow, during 40-50 min of contact time with 0.7-1.2% w/v of CSAC. The best values for CSAC loading and contact time to achieve the highest removal percentages are indicated by the yellow region. According to Oliver *et al.* (2018), the time and AC dosage implemented determine the adsorbent activity of the AC. The pigments' inherent antioxidants are absorbed and influence RBO's oxidation stability (Guedidi *et al.*, 2017; Islam *et al.*, 2018).

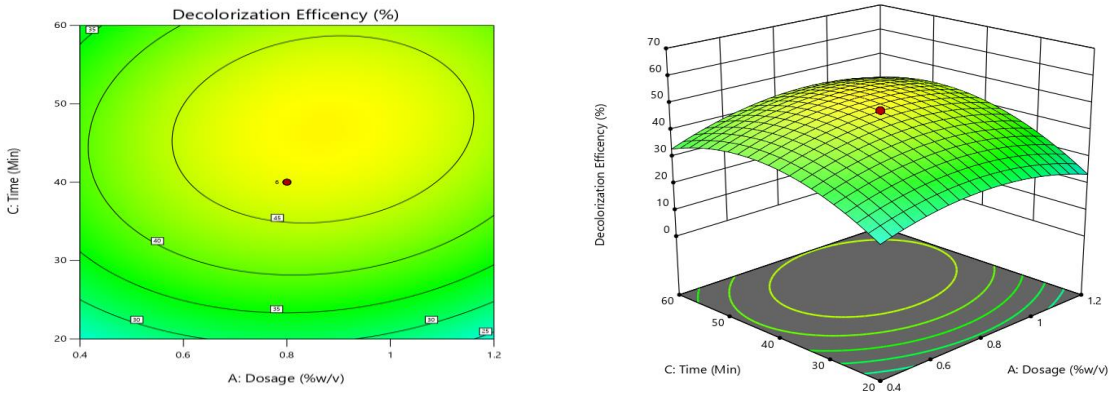

(a) (b)

Figure 3. (a) Contour plot interaction between dosage ($X1$) and contact time ($X3$) (b) 3D Surface Plot of response interaction between dosage ($X1$) and contact time ($X3$)

3.5 Response optimization of decolorization efficiency using CSAC

The optimum values of the optimum adsorption conditions were determined from the optimizer model in Design Expert Version 13. In this optimization analysis, the independent variables were selected to be (within the range), while the response was set as (maximum).

With a composite desirability score of 0.929, the model projected that a decolorization efficiency of 65.4% would be achieved. The optimum conditions for this percentage to be achieved are an adsorbent dosage of 0.85% w/v, temperature of 50^{o}C, and contact time of 43 min. A predicted percentage of 65.4% decolorization efficiency is guaranteed under the optimized conditions for efficient removal of impurities from RBO. Then, using the optimum conditions that were provided by RSM, the actual experimental decolorization efficiency achieved was 60.2%. The comparison between predicted and actual decolorization efficiency is demonstrated in **Table 6**.

Table 6. Predicted and actual comparison

Optimum adsorption conditions			**Response surface**		
Dosage of adsorbent, % w/v	Temperature, ^{o}C	Contact time, min	Predicted %	Actual, %	Error, %
0.85	50	43	65.4	60.2	8.7

According to Chen *et al.* (2013) and Mahmood *et al.* (2017), the optimization process of this study is considered tolerable, as evidenced by the comparatively small percentage error between the predicted and the actual values, which is less than 10%.

3.6 Color analysis

The RBO's color characteristics were assessed based on levels of redness, yellowness, and brightness resistance. To enable an effective comparison of the color values, the acquired color data were assembled in **Table 7**. According to Ren *et al.* (2018), the colorimeter parameter a^* (ranging from -80 to +80) is positive for reddish and negative for greenish

colors. Meanwhile, b^* runs from -80 to +80, with positive and negative values for yellowish and bluish colors, respectively. L^* is the estimated relative luminosity or brightness of the samples, ranging from 0 denoting black to 100 denoting white. Refined RBO color varies from pale yellow to dark green-brown, depending on the type of rice bran (Manjula & Subramanian, 2009). Seven samples were selected to be examined based on their percentage of decolorization efficiency (**Table 7**). The first sample, denoted as sample 1, is the sample that achieved the highest decolourization efficiency (61.1%), which represents the 8th run based on RSM actual experimental runs. Sample 2 represents the 2nd Run that achieved 57.3% decolorization. Sample 3 represents the 1st run that achieved a 47.5% decolorization efficiency. Sample 4 represented the 20th run that achieved 41.7%. Sample 5 and 6 (lowest percentage) represented the 17th run and 3rd run with percentages of 19.1 and 9.1%, respectively. Finally, sample 7 is the CRBO, as it was examined to compare the CRBO and the oils that went through the decolorization process to study the changes that occurred to them. The color and the percentage of decolorization were the main factors for selecting these samples to analyze further than the other samples.

As illustrated in **Table 7**, sample 7 which is for CRBO without any treatment by the CSAC adsorbent, had the lowest L^* value of 3.43. This low value is the nearest to 0, which indicates a black/dark appearance. On the other hand, sample 1 had a brightness L^* value of 16.45, which was the highest among treated samples, indicating that CSAC worked effectively in increasing this oil sample's lightness or brightness. Sample 2 with a L^* value of 16.03, falls behind sample 1. Samples 3, 4, 5, and 6 have significantly lower lightness values of 13.78, 4.88, 4.5, and 3.94, respectively, indicating that the decolorization was less effective for these samples as their brightness is lower than sample 1 and 2.

Table 7. Obtained color measurements for different RBO samples

Samples tested	L^*	a^*	b^*
Sample 1	16.45	-1.33	1.90
Sample 2	16.03	-0.37	3.75
Sample 3	13.78	1.18	1.93
Sample 4	4.88	3.32	2.23
Sample 5	4.50	4.95	2.89

Sample 6	3.94	3.23	1.17
Sample 7	3.43	6.30	10.49

Sample 7, the CRBO, had the highest a^* value of 6.3, indicating a strong red tint, which is typical due to the presence of carotenoids and other natural pigments. Among the treated samples, sample 1 had a^* value of -1.33, indicating a slight greenish shift, suggesting the successful decrease of the red pigments of carotenoids. Sample 2 has a^* value of -0.37, which is very close to neutral, indicating light green tint. Samples 3, 4, 5, and 6 had a^* values of 1.18, 3.32, 4.95, and 3.23, respectively, indicating varying degrees of red tint, with Sample 5 showing the strongest red tint among the treated samples, which is undesirable for the final RBO product. Since refined RBO tends to have a green undertone, sample 1 exhibited the desired and best results for decolorized RBO.

A lower b^* value for the refined RBO denotes a lighter yellow tint and less yellowness. Conversely, more yellowness and a more intense yellow color are indicated by a higher b^* value (Rekha *et al.*, 2014). Pathare *et al.* (2012) has also stated that fresh RBO has a positive b^* value and usually has a light yellowish tone. The CRBO sample 7, with a b^* value of 10.49, had the highest value, displaying the darkest yellow tint among all samples. Sample 6 and sample 1 on the other hand recorded the lowest b* values of 1.17 and 1.9, respectively. Sample 2 has more yellow pigments than sample 6 and 1, but still considerably less than the crude oil, with a b^* value of 3.75. The yellow tint in samples 3, 4, 5, and 6 ranges from 1.93 to 2.23, 2.89 to 1.17, respectively. Moreover, oxidation and component deterioration can occur as oils age or are processed, leading to an increase in the b^* value and a stronger yellow color. This is due to the formation of colored compounds as the oil degrades (Raza *et al.*, 2009).

Sample 1 demonstrated the most effective decolorization, with the highest lightness (L^*), a slight green shift in the red-green axis (b^*) and the lowest yellow tint (b^*). These results do align with Djaeni & Listyadevi (2019) findings, where their best extracted RBO had similar values of color measurements of lower a* and b*. On the other hand, sample 7, the untreated CRBO, exhibited the darkest color with the highest red and yellow tints, serving as a baseline for comparison.

4. Conclusion

All physical properties determined for the CSAC were in the typical range of the ACs that are used in industrial applications. The optimal combination of operating variables has been determined, and it was found that the optimized operating variable closely matches the quadratic model's prediction with an error percentage of 8.7. The optimal decolorization conditions based on optimization in RSM are an adsorbent dosage of 0.85% w/v, temperature of 50^{o}C, and contact time of 43 min. Based on the color analysis, it was determined that sample 1, which went through the conditions of the 8th run with an adsorbent dosage of 0.8 (w/v%), temperature of 30℃, and contact time of 40 min, was the most successful decolorization process out of all the runs that have been conducted. This result does show that under the right conditions, CSAC can be a very effective and promising adsorbent and aspires to offer a sustainable and efficient solution to the challenges faced in the decolorization of RBO mills. It should be emphasized that this study is intended solely for experimental purposes. The oil decolorized through this experimental methodology is not recommended for commercial use or consumption.

Acknowledgement

The authors pay their sincere gratitude to Universiti Malaysia Sabah (UMS) for providing necessary research facilities to accomplish this study.

Credit Author Statement

Conceptualization, S.M.A. and M.F.M.B.; methodology, M.F.M.B.; software, M.F.M.B.; validation, S.M.A. and M.F.M.B; formal analysis, M.F.M.B.; resources, S.M.A.; data curation, S.M.A. and M.F.M.B.; writing—original draft preparation, M.F.M.B.; writing—review and editing, S.M.A.; visualization, S.M.A. and M.F.M.B.; supervision, S.M.A.; project administration, S.M.A.

Conflict of interest

The authors declare no conflict of interest.

References

Aung, L. L. & Thiravetyan, P. (2014). Decolorization of rice bran oil: Adsorption of pigments on acid-activated kaolin. *Universities Research Journal*. 7, 327–338.

Butt, F.,Syed, M. A., & Shaik, F. (2020). Palm oil bleaching using activated carbon prepared from neem leaves and waste tea. *International Journal of Engineering Research and Technology*. 13(4), 620–624. https://doi.org/10.37624/ijert/13.4.2020.620-624

Chen, Y., Chen, W., Huang, B., & Huang, M. (2013). Process optimization of $K_2C_2O_4$-activated carbon from kenaf core using Box–Behnken design. *Chemical Engineering Research & Design*. 91(9), 1783–1789. https://doi.org/10.1016/j.cherd.2013.02.024

Chetima, A., Wahabou, A., Zomegni, G., Ntieche R. A., & Bup N, D. (2018). Bleaching of neutral cotton seed oil using organic activated carbon in a batch system: Kinetics and adsorption isotherms. *Processes*. 6(3), 22. https://doi.org/10.3390/pr6030022

Dąbrowski, A., Podkościelny, P., Hubicki, Z., & Barczak, M. (2005). Adsorption of phenolic compounds by activated carbon-a critical review. *Chemosphere*. *58*(8), 1049–1070. https://doi.org/10.1016/j.chemosphere.2004.09.067

Damayanti, A., Harianingsih, Ash, Z., Bahlawan, S., Shohib, Q., Dillah, Dinara, Y., Dewi, S., Kristi, S., Prasetyo, R., Dewi, S., Kristi, Y., & Prasetyo, S. (2023). Optimization of rice bran oil bleaching via carotenoid adsorption onto activated carbon using response surface methodology (RSM). *Reaktor*. *23*(2), 53–61. https://doi.org/10.14710/reaktor

Djaeni, M., & Listyadevi, Y. L. (2019). The ultrasound-assisted extraction of rice bran oil with n-hexane as a solvent. *Journal of Physics: Conference Series*. 1295, 012027. https://doi.org/10.1088/1742-6596/1295/1/012027

Efeovbokhan, V. E., Alagbe, E. E., Odika, B., Babalola, R., Oladimeji, T. E., Abatan, O. G., & Yusuf, E. O. (2019). Preparation and characterization of activated carbon from plantain peel and coconut shell using biological activators. *Journal of Physics: Conference Series*. 1378, 032035. https://doi.org/ 10.1088/1742-6596/1378/3/032035

El Haddad, M., Slimani, R., Mamouni, R., ElAntri, S., & Lazar, S. (2013). Removal of two textile dyes from aqueous solutions onto calcined bones. *Journal of the Association of Arab Universities for Basic and* Applied. 14(1), 51–59. https://doi.org/10.1016/j.jaubas.2013.03.002

Engelmann, J. I., Ramos, L. P., Crexi, V. T., & Morais, M. M. (2016). Degumming and neutralization of rice bran oil. *Journal of Food Process Engineering*. 40(2), e12362. https://doi.org/10.1111/jfpe.12362

Gao, W. & Fatehi, P. (2018). Fly ash based adsorbent for treating bleaching effluent of kraft pulping process. *Separation and Purification Technology*. 195, 60–69. https://doi.org/10.1016/j.seppur.2017.12.002.

Ghahjaverestani, S. T., Gharachorloo, M., & Ghavami, M. (2022). Application of coconut fiber and shell in the bleaching of soybean oil. *Grasas Y Aceites*. *73*(3), e471. https://doi.org/10.3989/gya.0781211

Guedidi, H., Reinert, L., Soneda, Y., Bellakhal, N., & Duclaux, L. (2017) Adsorption of ibuprofen from aqueous solution on chemically surface-modified activated carbon cloths. *Arabian Journal of Chemistry*. 10, S3584–S3594. https://doi.org/10.1016/j.arabjc.2014.03.007

Guliyev, N. G., Ibrahimov, H. J., Alekperov, J. A., Amirov, F. A., & Ibrahimova, Z. M. (2018). Investigation of activated carbon obtained from the liquid products of pyrolysis in sunflower oil bleaching process. *International Journal of Industrial Chemistry*. 9(3), 277–284. https://doi.org/10.1007/s40090-018-0156-1

Ifa, L., Wiyani, L., Nurdjannah, N., Ghalib, A. M. T., Ramadhaniar, S., & Kusuma, H. S. (2021). Analysis of bentonite performance on the quality of refined crude palm oil's color, free fatty acid and carotene: The effect of bentonite concentration and contact time. *Heliyon*. 7(6), e07230. https://doi.org/10.1016/j.heliyon.2021.e07230

Ikumapayi, O. M., Akinlabi, E. T., Majumdar, J. D., & Akinlabi, S. A. (2020). applications of coconut shell ash/particles in modern manufacturing: A case study of friction stir processing. Modern Manufacturing Processes. *Woodhead Publishing Reviews: Mechanical Engineering Series*. 69–95. https://doi.org/10.1016/b978-0-12-819496-6.00004-x

Islam, M. A., Tan, Y. L., Islam, M. A., Romić, M., Hameed, B. H. (2018). Chitosan–Bleaching Earth Clay Composite as an Efficient Adsorbent for Carbon Dioxide Adsorption: Process Optimization. *Colloids and Surfaces A: Physicochemical and Engineering Aspects*. 554, 9–15. https://doi.org/10.1016/j.colsurfa.2018.06.021

Jeyakumar, R. P. S. & Chandrasekaran, V. (2014). Preparation and characterization of activated carbons derived from marine green algae Ulva fasciata sp. *Asian Journal of Chemistry*. *26*(9), 2545–2549. https://doi.org/10.14233/ajchem.2014.15723

Liu, R., Shi, L., Zhang, Z., Zhang, T., Lu, M., Chang, M., Jin, Q., & Wang, X. (2019). Effect of refining process on physicochemical parameters, chemical compositions and in vitro antioxidant activities of rice bran oil. *LWT*. 109, 26–32. https://doi.org/10.1016/j.lwt.2019.03.096

Manjula, S., & Subramanian, R. (2009). Simultaneous degumming, dewaxing and decolorizing crude rice bran oil using nonporous membranes. *Separation and Purification Technology*. 66(2), 223–228. https://doi.org/10.1016/j.seppur.2009.01.004

Mahmood, T., Ali, R., Naeem, A., Hamayun, M., & Aslam, M. (2017). Potential of used *Camellia sinensis* leaves as precursor for activated carbon preparation by chemical

activation with H_3PO_4; optimization using response surface methodology. *Process Safety and Environmental Protection*. 109, 548–563. https://doi.org/10.1016/j.psep.2017.04.024.

Mopoung, S., Moonsri, P., Palas, W., & Khumpai, S. (2015). Characterization and properties of activated carbon prepared from tamarind seeds by KOH activation for Fe(III) adsorption from aqueous solution. *The Scientific World Journal*. 2015, 1–9. https://doi.org/10.1155/2015/415961

Ofulue, E. I. O., Adekola, F. A., & Adimula, V. O. (2020). Preparation of activated carbon from teak leaves for the decolorization of palm oil. *Journal of Chemical Society of Nigeria*. 45(5), 1–8 https://doi.org/10.46602/jcsn.v45i5.519

Oliver, J. K., Berkelmans, R., & Eakin, C. M. (2018). Coral Bleaching in Space and Time. *Ecological Studies*. 27–49. https://doi.org/10.1007/978-3-319-75393-5_3

Paisan, S., Chetpattananondh, P., & Chongkhong, S. (2017). Assessment of water degumming and acid degumming of mixed algal oil. *Journal of Environmental Chemical Engineering*. 5(5), 5115–5123. https://doi.org/10.1016/j.jece.2017.09.045

Pathare, P. B., Opara, U. L., & Al-Said, F. A. J. (2012). Colour measurement and analysis in fresh and processed foods: A review. *Food and Bioprocess Technology*. 6(1), 36–60. https://doi.org/10.1007/s11947-012-0867-9

Phannasorn, W., Pharapirom, A., Thiennimitr, P., Guo, H., Ketnawa, S., & Wongpoomchai, R. (2022). Enriched riceberry bran oil exerts chemopreventive properties through anti-inflammation and alteration of gut microbiota in carcinogen-induced liver and colon carcinogenesis in rats. *Cancers*. 14(18), 4358–4358. https://doi.org/10.3390/cancers14184358

Pohndorf, R. S., Cadaval, T. R. S., & Pinto, L. A. A. (2016). Kinetics and thermodynamics adsorption of carotenoids and chlorophylls in rice bran oil bleaching. *Journal of Food Engineering*. 185, 9–16. https://doi.org/10.1016/j.jfoodeng.2016.03.028

Punia, S., Kumar, M., Siroha, A. K., & Purewal, S. S. (2021). Rice Bran Oil: Emerging trends in extraction, health benefit, and its industrial application. *Rice Science*. 28(3), 217–232. https://doi.org/10.1016/j.rsci.2021.04.002

Punsuwan, N., Tangsathitkulchai, C., & Takarada, T. (2015). Low temperature gasification of coconut shell with co2 and koh: effects of temperature, chemical loading, and introduced carbonization step on the properties of syngas and porous carbon product. *International Journal of Chemical Engineering*. 2015(1), e481615. https://doi.org/10.1155/2015/481615

Rahman, A. N. F., Asfar, M., Suwandi, N., & Amir, M. R. R. (2019). The effect of grain germination to improve rice quality. *IOP conference series. Earth and environmental science*. 355 (1), 012110–012110. https://doi.org/10.1088/1755-1315/355/1/012110

Raza, S. A., Rashid, A., Qureshi, F. A., Asim, M. F., & William, J. (2009). Analytical investigation of oxidative deterioration of Sunflower Oil stored under different conditions. *Biharean Biologist.* 3(2), 93–97

Rekha, B., Lokesh, B. R., & Krishna, A. G. G. (2014). Chemistry of color fixation in crude, physically refined and chemically refined rice bran oils upon heating. *Journal of the American Oil Chemists' Society*. 91(10), 1665–1676. https://doi.org/10.1007/s11746-014-2520-4

Ren, J. N., Zhang, Y., Fan, G., Wang, M. P., Zhang, L. L., Yang, Z. Y., & Pan, S. Y. (2018). Study on the optimization of the decolorization of orange essential oil. *Food Science and Biotechnology*. 27(4), 929–938. https://doi.org/10.1007/s10068-018-0354-9

Siragi D. B. M., Desmecht, D., Hima, H., Mamane, O., & Natatou, I. (2021). Optimization of activated carbons prepared from *Parinari macrophylla* shells. *Materials Sciences and Applications*. 12(5), 207–222. https://doi:10.4236/msa.2021.125014

Somashekhar, T. M., Naik, P., Nayak, V., Mallikappa, & Rahul, S. (2018). Study of mechanical properties of coconut shell powder and tamarind shell powder reinforced with epoxy composites. *IOP Conference Series: Materials Science and Engineering*. 376, 012105. https://doi.org/10.1088/1757-899x/376/1/012105

Sun, B., Gao, P., Yu, H., Dong, Z., Yin, J., Zhong, W., HU C., He D., & Wang, X. (2023). Optimization of composite decolorizer efficacy based on decolorization efficiency, toxicity, and nutritional value of rice bran oil. *Journal of Oleo Science*. 72(8), 755-765. https://DOI: 10.5650/jos.ess23050

Tan, I. A. W., Abdullah, M. O., Lim, L. L. P., & Yeo, T. H. C. (2017). Surface modification and characterization of coconut shell-based activated carbon subjected to acidic and alkaline treatments. *Journal of Applied Science & Process Engineering*. *4*(2), 186–194. https://doi.org/10.33736/jaspe.435.2017

Tong, C. & Bao, J. (2019). 5 - Rice lipids and rice bran oil. *Rice (Fourth Edition) Chemistry and Technology*. 131–168. https://doi.org/10.1016/b978-0-12-811508-4.00005-8

Worasith, N., Goodman, B. A., Jeyashoke, N., Thiravetyan, P. (2011). Decolorization of Rice Bran Oil Using Modified Kaolin. *Journal of the American Oil Chemists' Society*. 88 (12), 2005–2014. https://doi.org/10.1007/s11746-011-1872-2

Zulkania, A., Hanum, G. F., & Sri Rezki, A. (2018). The potential of activated carbon derived from bio-char waste of bio-oil pyrolysis as adsorbent. *MATEC Web of Conferences*, *154*, 01029. https://doi.org/10.1051/matecconf/201815401029